

Cyclic CO₂ capture characteristics of a pellet derived from sol-gel CaO powder with Ca₁₂Al₁₄O₃₃ support

Cong Luo^{*,†}, Ying Zheng^{*}, Yongqing Xu^{*}, Haoran Ding^{*}, Chuguang Zheng^{*}, Changlei Qin^{**}, and Bo Feng^{***}

^{*}State Key Laboratory of Coal Combustion, Huazhong University of Science and Technology, Wuhan 430074, China

^{**}College of Power Engineering, Chongqing University, Chongqing 400044, China

^{***}School of Mechanical and Mining Engineering, The University of Queensland, St Lucia, QLD 4072, Australia

(Received 3 June 2014 • accepted 27 September 2014)

Abstract—A novel calcium-based pellet was prepared by extrusion of sol-gel CaO powder and cement with high aluminum-based content. Limestone was used for comparison. The cyclic CO₂ capture performance and carbonation kinetics of the sorbents were investigated in a thermogravimetric analyzer (TGA). The changes in phase and microstructure were characterized by X-ray diffraction (XRD), scanning electron microscopy (SEM) and Brunauer Emmet Teller (BET) surface area, respectively. The results indicate that the pellet consisted of CaO and Ca₁₂Al₁₄O₃₃ after initial calcination. Limestone reactivity decreased dramatically with the increase in the cycle number, whereas the pellet showed a relatively stable cyclic CO₂ capture performance with high reactivity. The CO₂ capture capacity of the pellet achieved 0.43 g CO₂/g sorbent after 50 cycles at 650 °C and 850 °C for carbonation and calcination, respectively. Moreover, the pellet obtained fast carbonation rates with slight decay after multiple cycles. The porous microstructure of the pellet contributed to the high reactivity of the sorbent during high temperature reactions, and the support material of Ca₁₂Al₁₄O₃₃ enhanced the cyclic durability of the calcium-based sorbents.

Keywords: CO₂ Capture, Calcium Looping, Pellet, Sol-gel, Limestone

INTRODUCTION

The rapid increase in carbon dioxide (CO₂) concentration in the atmosphere has attracted much concern because it considerably contributes to global warming. Thus, CO₂ capture and storage have been paid much attention globally [1-6]. The cyclic carbonation/calcination reactions of calcium-based sorbents for CO₂ capture, also called calcium looping, have recently been identified as one of the best CO₂ capture technologies [7-10]. However, calcium looping is limited by the loss in the capacity of natural calcium-based sorbents as carbonation/calcination cycle numbers increase [11-14]. The CO₂ capture capacity of natural limestone decreases from 0.61 g CO₂/g sorbent during the first cycle to 0.18 g CO₂/g sorbent during the 10th cycle at 850 °C and 650 °C for calcination and carbonation, respectively [15]. Therefore, new preparation methods need to be developed to enhance the cyclic performance of the calcium-based sorbents [16-24]. Recent studies have proposed a sol-gel process to synthesize calcium-based sorbents with high cyclic reactivity [25-31]. CaO powder prepared through the sol-gel process showed that well-dispersed particles with an average size of approximately 200 nm formed within the sorbent with CO₂ capture capacity of the powder at 0.51 g CO₂/g sorbent during 20th cycle [32].

However, CaO powder with an average size of ~200 nm is not suitable for current large-scale calcium looping system and should

be further prepared into pellets. This study is an extension of previous works by the authors and is conducted to manufacture a calcium-based pellet with high reactivity for cyclic carbonation/calcination reactions. Moreover, because calcium-based sorbents supported by aluminum-based materials have shown high durability after long-term cyclic reactions [33-37], a cement with high aluminum-based content was selected as the bonding and supporting material to manufacture calcium-based pellet. The effects of the phase transformation of aluminum-based support and the morphological changes inside the pellet during cyclic high-temperature reactions on the CO₂ capture performance of the sorbent were also discussed.

EXPERIMENTAL SECTION

1. Materials and Sorbent Preparation

The sol-gel CaO powder (denoted as SG CaO) was prepared according to the procedure in the authors' previous study [32]. The predetermined amounts of analytical reagent-grade metal nitrate tetrahydrate and citric acid monohydrate were added to distilled water at a water-to-metal ion molar ratio of 40 : 1 and a citric acid-to-metal ion molar ratio of 1 : 1. Then, the mixture was continuously stirred and kept at 80 °C in an electrically heated thermostatic water bath for 7 h to form a translucent sol. Subsequently, the sol was placed at room temperature for 18 h in a sealed container to form a wet gelatin before it was placed in a drying oven at 80 °C for 5 h and then dried at 110 °C for another 12 h until a dry gelatin was formed. At last, the dry gelatin was placed into a muffle furnace at 600 °C for few seconds, and then the sample was

[†]To whom correspondence should be addressed.

E-mail: cluo@hust.edu.cn

Copyright by The Korean Institute of Chemical Engineers.

calcined at 700 °C in a tube furnace for 20 min in an N₂ atmosphere to burn out the carbonate.

The as-prepared SG CaO powder and one cement powder produced by Kerneos Aluminate Technologies were used to synthesize the calcium-based pellet as follows. The average particle size of the cement powder is ~35 μm. The predetermined SG CaO and the cement were physically mixed with a mass ratio of 3:1. The reason for choosing this ratio is that Li et al. suggested that CaO/Ca₁₂Al₁₄O₃₃ (75/25 wt%) has excellent regeneration capacity in cyclic use [38]. The mixture was then extruded to long cylinders through an extruder with a die (which has one hole with a diameter of 2 mm). During extrusion, a little water was added to help solidify the mixture and improve the hardness of the pellet. The pellet was subjected to cyclic carbonation/calcination performance test after being dried overnight at 110 °C and calcined at 900 °C in a tube furnace for 3 h under an N₂ atmosphere.

A natural Australian limestone purchased from Agricola Mining Pty Ltd was also used for comparison. The elemental composition analysis with an X-ray fluorescence (XRF) spectrometer indicated that the limestone after complete decomposition of carbonate was composed of CaO 96.31%, MgO 1.36%, SiO₂ 0.71%, Al₂O₃ 0.61%, Fe₂O₃ 0.43%, SO₃ 0.31%, and others 0.26%. Before testing, the pellet and limestone were pulverized and sieved with particle size in the range of 250–400 μm.

2. Characterization and CO₂ Capture Testing

The phase composition of the samples was determined by X-ray diffraction (XRD, PANalytical B.V.) with Cu Kα radiation (λ = 0.1542 nm) within the 2θ range of 20°–70° and a scanning speed of 0.1°/s. The microstructure of the calcined samples was investigated in a high vacuum by field-emission scanning electron microscopy (SEM, Sirion200, FEI Inc.) system with 5 kV of accelerating voltage. The pore structure parameters of the calcined sample were examined from N₂ adsorption and desorption isotherms, measured at the temperature of liquid N₂ (Micromeritics ASAP 2020-M). The surface area data were calculated from the Brunauer Emmet Teller (BET) equations.

The cyclic carbonation/calcination performance of the calcium-based sorbents was investigated in a thermogravimetric analyzer (TGA, Cahn 121). The testing procedure was as follows: about 20 mg of the sample was placed in a quartz sample pan and heated from room temperature to 850 °C at a rate of 20 °C/min in a N₂ flow of 100 ml/min under atmosphere pressure and maintained at 850 °C for 10 min to fully decompose CaCO₃. Subsequently, the sample was cooled to 650 °C in N₂, and then, the cyclic carbonation/calcination reactions began. The samples were carbonated at 650 °C for 15 min in 15 vol% CO₂ balanced by N₂, and calcined at 850 °C for 10 min in N₂. Both cooling and heating processes of TGA were conducted in N₂ at heating or cooling rate of 20 °C/min.

RESULTS AND DISCUSSION

1. X-ray Diffraction Analysis

The chemical compositions of SG CaO, cement and the pellet derived from SG CaO and cement were analyzed by X-ray diffraction (XRD) as shown in Fig. 1. The main phase of the SG CaO powder was CaO, and the main phases of cement were CaAl₂O₄ and

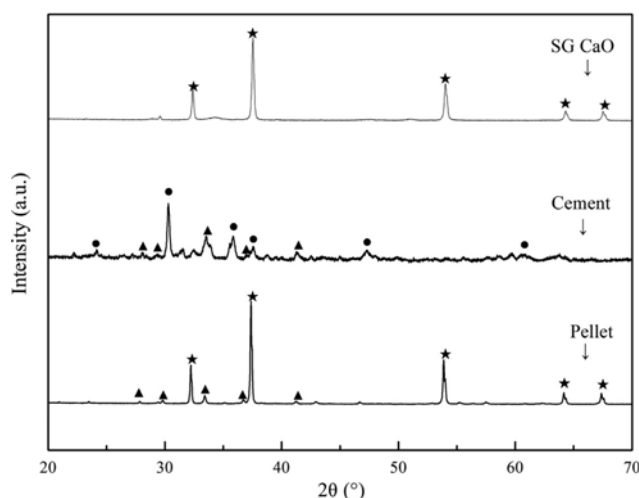


Fig. 1. XRD patterns of SG CaO, cement and the pellet derived from SG CaO and cement after calcination under N₂ atmosphere (★ CaO, ● CaAl₂O₄, and ▲ Ca₁₂Al₁₄O₃₃).

Ca₁₂Al₁₄O₃₃. Previous studies showed that Ca₁₂Al₁₄O₃₃ incorporation is highly beneficial to CaO-based sorbent for capturing CO₂, especially after long-term cyclic carbonation/calcination reactions [16,36,39,40]. This phenomenon is due to the fact that the inert Ca₁₂Al₁₄O₃₃ functioned as a framework material among the CaO grains, so it could resist high-temperature sintering of CaO grains and enhance the cyclic reactivity of the sorbents. Therefore, transforming CaAl₂O₄ into Ca₁₂Al₁₄O₃₃ is advantageous in the manufacture of an excellent calcium-based sorbent with aluminum-based support.

Li et al. showed that the inert phase of Ca₁₂Al₁₄O₃₃ was formed when a calcination temperature of 800–1,000 °C was applied in the sorbent preparation stage [41]. In this study, the sorbent was calcined at 900 °C under N₂ for 3 h after SG CaO and cement were extruded into the pellet. The main phases of the pellet were CaO and Ca₁₂Al₁₄O₃₃, and the CaAl₂O₄ phase disappeared (Fig. 1). This finding indicates that most of CaAl₂O₄ reacted with CaO as follows:



These results are consistent with those of Li et al.

2. CO₂ Capture Performance of the Sorbents

The CO₂ capture performance of the pellet and limestone is compared in Fig. 2. The CO₂ capture capacity of the limestone decreased dramatically with the increase in cycle number: 0.54 and 0.09 g CO₂/g sorbent during the first and fiftieth cycle, respectively. However, the CO₂ capture capacity of the pellet remained relatively stable during the cyclic carbonation/calcination reactions: 0.52 and 0.43 g CO₂/g sorbent during the first and fiftieth cycle, respectively. In the authors' previous study, CaO powder derived from a sol-gel process achieved a CO₂ capture capacity of 0.37 g CO₂/g sorbent during the twentieth cycle under the same reaction conditions used in the current research [32]. This result indicates that the pellet exceeded its precursor in cyclic CO₂ capture performance. An important reason could be that the inert support material of Ca₁₂Al₁₄O₃₃ inside the pellet might have served as the framework among the

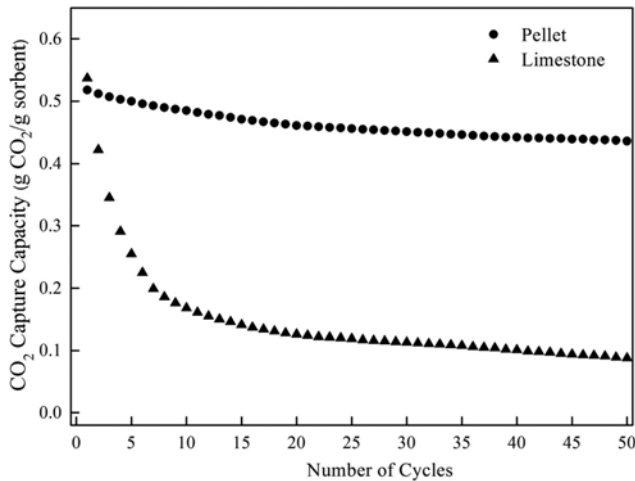


Fig. 2. Cyclic CO₂ capture performance of the pellet and limestone.

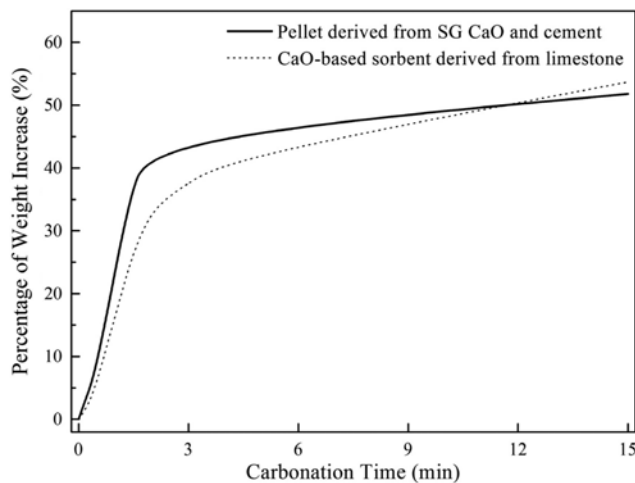


Fig. 3. Carbonation kinetics of the pellet and limestone during the first cycle.

CaO grains, thereby enhancing the cyclic durability of the sorbent. Note also that most reactivity decay of the two sorbents occurred within 20 cycles. Further investigations focus on the different characteristics of the sorbents during the first and twentieth cycle.

The carbonation kinetics of the two sorbents during the first cycle is shown in Fig. 3. Both sorbents exhibited high carbonation rates during the initial chemical reaction control stage, which was followed by an abrupt shift to relatively lower carbonation rates during product layer diffusion. The initial carbonation rates of the pellet were faster than those of limestone, because the pellet had smaller crystallites that could have contributed to the rapid gas-solid reaction. However, the final increase in the mass of the pellet was a slightly smaller than that of the limestone after 15 min carbonation. This result does not suggest that CO₂ diffused through the product layer of limestone more easily, because CaO content in the pellet was considerably less than that of CaO in the limestone. A calcium-based sorbent with 25 wt% cement could obtain less than 58.9% increase in mass ratio during carbonation. The final mass increase in the mass of the pellet was over 90% of its maximum value.

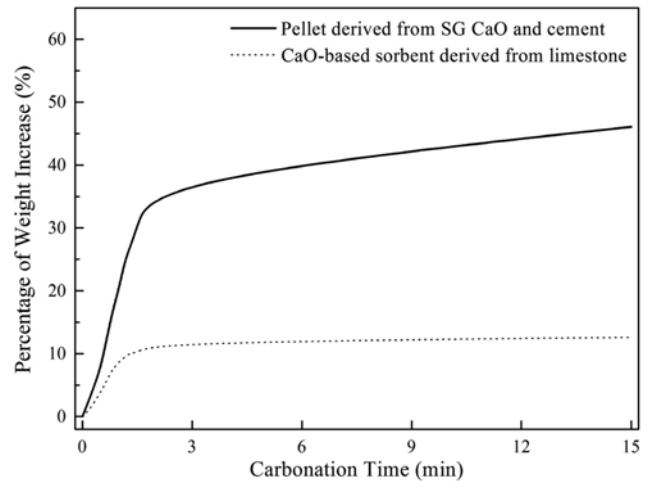


Fig. 4. Carbonation kinetics of the pellet and limestone during the 20th cycle.

The carbonation kinetics of the two sorbents during the 20th cycle is shown in Fig. 4. The carbonation kinetics of the two sorbents also contained two stages: a chemical reaction control stage and a product layer diffusion stage. The pellet achieved higher carbonation conversion than the limestone at the end of the chemical reaction control stage. Contrary to the results in Fig. 3, the reaction rates of limestone showed rapid decay from cycles 1 to 20, whereas the pellet showed slight decay in reaction rates.

3. Discussion

SEM images of the pellet and the limestone after initial calcination and after 20 cycles are shown in Fig. 5. Both sorbents exhibited rough surfaces with numerous pores after initial calcination [Figs. 5(a) and (b)]. According to Bhatia, a porous surface is beneficial for the carbonation reaction [42], indicating that both sorbents absorbed CO₂ with high efficiency in the present study. However, the crystallites of the pellet were smaller than those of the limestone, according to a previous study that has shown a sorbent with small crystallites exhibits fast reaction kinetics [43]. After 20 cycles, the pellet and limestone showed totally different microstructures [Figs. 5(c) and (d)]. The pellet surface was still rough and contained many pores. By contrast, sintering of the limestone was vigorous, and most of the pores disappeared compared with its initial status. Therefore, the microstructure of the pellet remained relatively stable during the high-temperature reactions. The BET surface area data are given in Table 1. The pellet showed much larger specific surface area than the limestone after initial calcinations, as well as after 20 cycles. The results are consistent with previous study which suggested that the BET surface area affected the carbonation conversion at chemical controlled reaction stage [27,44].

In general, the pellet derived from sol-gel CaO powder with Ca₁₂Al₁₄O₃₃ support material is a promising sorbent for application in calcium looping technology. The sol-gel process has been previously shown by the authors to contribute to the preparation of well-dispersed CaO powders (approximately 200 nm in particle size). The sol-gel CaO also showed high reactivity during high-temperature reactions [17]. The extrusion method applied in the current study was based on a physical method, and it did not destroy the chemi-

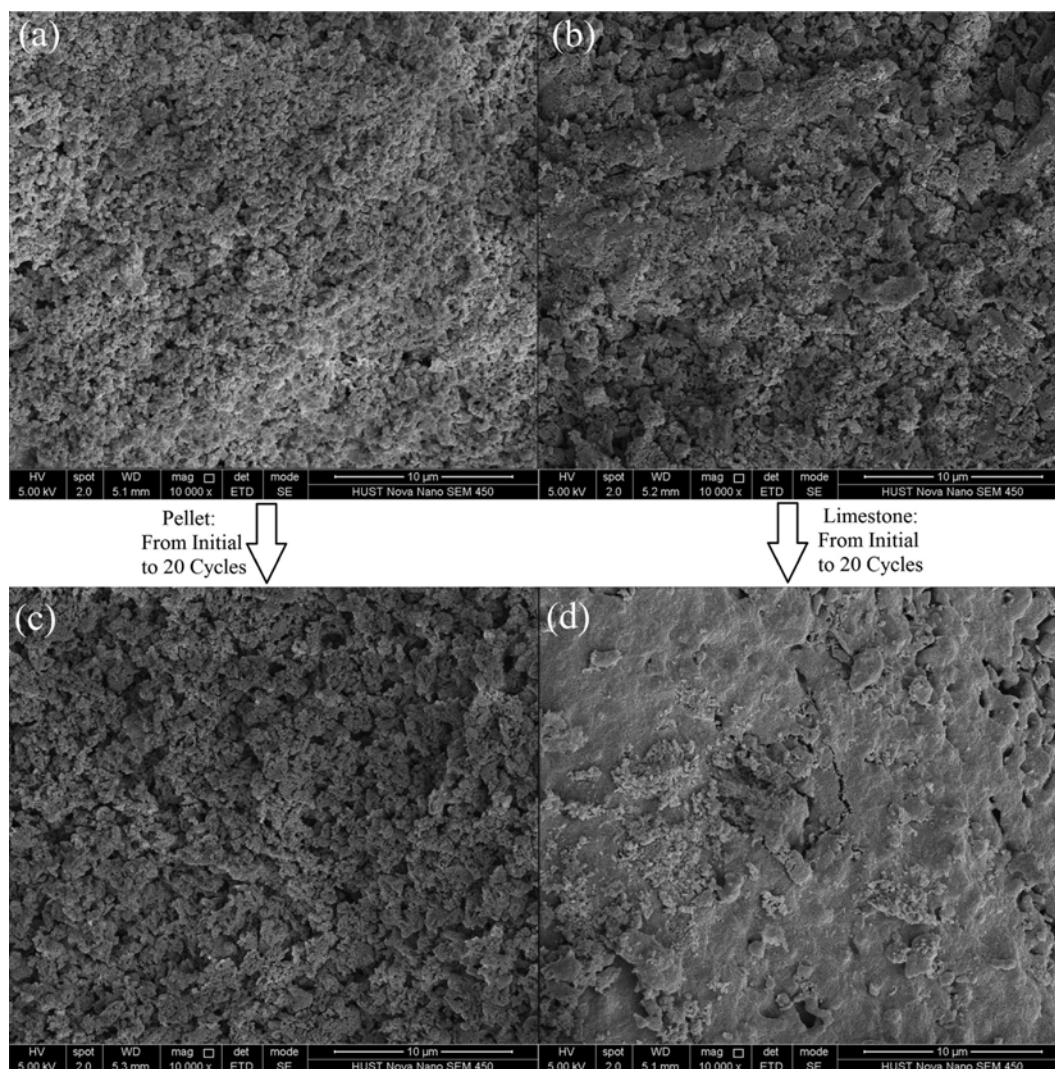


Fig. 5. SEM images of the pellet and limestone (calcined sample): (a) pellet after initial calcination, (b) limestone after initial calcination, (c) pellet after 20 cycles, (d) limestone after 20 cycles.

Table 1. BET surface areas of the pellet and limestone after initial calcination and 20 cycles

	Pellet	Limestone
Initial	16.4 m ² /g	13.1 m ² /g
Cycle 20	9.8 m ² /g	3.2 m ² /g

cal characteristics of the sol-gel CaO powders. Therefore, the high reactivity property of the sol-gel CaO powders was retained by the pellet. The addition of cement, which was transformed into Ca₁₂Al₁₄O₃₃, enhanced the cyclic durability of the calcium-based sorbents. Hence, the pellet obtained an excellent CO₂ capture performance during cyclic carbonation/calcination reactions.

CONCLUSIONS

The novel calcium-based pellet prepared by extrusion of sol-gel CaO powders and cement showed a porous microstructure that remained relatively stable during cyclic reactions. The CO₂ capture

capacity and the carbonation rate of the pellet were higher than those of limestone after multiple cycles. The pellet showed high reactivity with respect to its precursor of sol-gel CaO powders, and the inert support material of Ca₁₂Al₁₄O₃₃ enhanced the cyclic durability of the sorbents. Thus, the pellet exhibited an excellent CO₂ capture performance for calcium looping cycles.

ACKNOWLEDGEMENTS

The authors are grateful to China Postdoctoral Science Foundation funded project (2014M550391), National Natural Science Foundation of China (51276078), Foundation of State Key Laboratory of Coal Combustion (FSKLCC1405), and Analytical and Testing Center of HUST for XRD and SEM measurements.

REFERENCES

1. N. MacDowell, N. Florin, A. Buchard, J. Hallett, A. Galindo, G. Jackson, C. S. Adjiman, C. K. Williams, N. Shah and P. Fennell, *Energy*

- Environ. Sci.*, **3**, 1645 (2010).
2. F.-C. Yu, N. Phalak, Z. Sun and L.-S. Fan, *Ind. Eng. Chem. Res.*, **51**, 2133 (2012).
 3. H. An, T. Song, L. Shen, L. Zhang and B. Feng, *Ind. Eng. Chem. Res.*, **51**, 13046 (2012).
 4. M. Zaman and J. H. Lee, *Korean J. Chem. Eng.*, **30**, 1497 (2013).
 5. U. Zahid, Y. Lim, J. Jung and C. Han, *Korean J. Chem. Eng.*, **28**, 674 (2011).
 6. J. H. Choi, C. K. Yi, S. H. Jo, H. J. Ryu and Y. C. Park, *Korean J. Chem. Eng.*, **31**, 194 (2014).
 7. C. C. Dean, J. Blamey, N. H. Florin, M. J. Al-Jeboori and P. S. Fennell, *Chem. Eng. Res. Des.*, **89**, 836 (2011).
 8. J. Blamey, E. J. Anthony, J. Wang and P. S. Fennell, *Prog. Energy Combust.*, **36**, 260 (2010).
 9. S. Wang, S. Fan, Y. Zhao, L. Fan, S. Liu and X. Ma, *Ind. Eng. Chem. Res.*, **53**, 10457 (2014).
 10. C. Q. Cao, K. Zhang, C. C. He, Y. A. Zhao and Q. J. Guo, *Chem. Eng. Sci.*, **66**, 375 (2011).
 11. J. C. Abanades, *Chem. Eng. J.*, **90**, 303 (2002).
 12. B. Feng, W. Q. Liu, X. Li and H. An, *Energy Fuels*, **20**, 2417 (2006).
 13. F. Fang, Z. S. Li and N. S. Cai, *Korean J. Chem. Eng.*, **26**, 1414 (2009).
 14. T. Wittoon, *Ceram. Int.*, **37**, 3291 (2011).
 15. G. S. Grasa and J. C. Abanades, *Ind. Eng. Chem. Res.*, **45**, 8846 (2006).
 16. W. Q. Liu, H. An, C. L. Qin, J. J. Yin, G. X. Wang, B. Feng and M. H. Xu, *Energy Fuels*, **26**, 2751 (2012).
 17. R. Y. Sun, Y. J. Li, H. L. Liu, S. M. Wu and C. M. Lu, *Appl. Energy*, **89**, 368 (2012).
 18. V. Manovic and E. J. Anthony, *Environ. Sci. Technol.*, **43**, 7117 (2009).
 19. C.-C. Li, U.-T. Wu and H.-P. Lin, *J. Mater. Chem. A*, **2**, 8252 (2014).
 20. X. Zhang, Z. Li, Y. Peng, W. Su, X. Sun and J. Li, *Chem. Eng. J.*, **243**, 297 (2014).
 21. J. Yin, C. Qin, B. Feng, L. Ge, C. Luo, W. Liu and H. An, *Energy Fuels*, **28**, 307 (2014).
 22. C. Qin, J. Yin, C. Luo, H. An, W. Liu and B. Feng, *Chem. Eng. J.*, **228**, 75 (2013).
 23. Y. J. Li, R. Y. Sun, H. L. Liu and C. M. Lu, *Ind. Eng. Chem. Res.*, **50**, 10222 (2011).
 24. H. C. Chen, C. S. Zhao, L. B. Duan, C. Liang, D. J. Liu and X. P. Chen, *Fuel Process. Technol.*, **92**, 493 (2011).
 25. C. Luo, Y. Zheng, N. Ding, Q. L. Wu, G. A. Bian and C. G. Zheng, *Ind. Eng. Chem. Res.*, **49**, 11778 (2010).
 26. M. Broda, A. M. Kierzkowska and C. R. Müller, *ChemSusChem*, **5**, 411 (2012).
 27. A. Akgornpeak, T. Wittoon, T. Mungcharoen and J. Limtrakul, *Chem. Eng. J.*, **237**, 189 (2014).
 28. E. T. Santos, C. Alfonsín, A. J. S. Chambel, A. Fernandes, A. P. Soares Dias, C. I. C. Pinheiro and M. F. Ribeiro, *Fuel*, **94**, 624 (2012).
 29. P. Xu, M. Xie, Z. Cheng and Z. Zhou, *Ind. Eng. Chem. Res.*, **52**, 12161 (2013).
 30. S. D. Angeli, C. S. Martavaltzi and A. A. Lemionidou, *Fuel*, **127**, 62 (2014).
 31. A. M. Kierzkowska and C. R. Muller, *Energy Environ. Sci.*, **5**, 6061 (2012).
 32. C. Luo, Y. Zheng, C. G. Zheng, J. J. Yin, C. L. Qin and B. Feng, *Int. J. Greenh. Gas Con.*, **12**, 193 (2013).
 33. Z. S. Li, Y. Liu and N. S. Cai, *Chem. Eng. Sci.*, **89**, 235 (2013).
 34. C. Luo, Y. Zheng, N. Ding, Q. L. Wu and C. G. Zheng, *Chin. Chem. Lett.*, **22**, 615 (2011).
 35. Z. Zhou, Y. Qi, M. Xie, Z. Cheng and W. Yuan, *Chem. Eng. Sci.*, **74**, 172 (2012).
 36. K. Wang, X. Guo, P. F. Zhao and C. G. Zheng, *Appl. Clay Sci.*, **50**, 41 (2010).
 37. V. Manovic and E. J. Anthony, *Ind. Eng. Chem. Res.*, **49**, 6916 (2010).
 38. Z. S. Li, N. S. Cai, Y. Y. Huang and H. J. Han, *Energy Fuels*, **19**, 1447 (2005).
 39. C. S. Martavaltzi and A. A. Lemionidou, *Ind. Eng. Chem. Res.*, **47**, 9537 (2008).
 40. V. Manovic and E. J. Anthony, *Ind. Eng. Chem. Res.*, **48**, 8906 (2009).
 41. Z. S. Li, N. S. Cai and Y. Y. Huang, *Ind. Eng. Chem. Res.*, **45**, 1911 (2006).
 42. S. K. Bhatia and D. D. Perlmutter, *AIChE J.*, **29**, 79 (1983).
 43. C. Luo, Q. W. Shen, N. Ding, Z. X. Feng, Y. Zheng and C. G. Zheng, *Chem. Eng. Technol.*, **35**, 547 (2012).
 44. T. Wittoon, T. Mungcharoen and J. Limtrakul, *Appl. Energy*, **118**, 32 (2014).